200830037A

厚生労働科学研究費補助金

エイズ対策研究事業

エイズ多剤併用療法中のリザーバーの特定および選択的障害に関する研究

平成２０年度　総括研究報告書

研究代表者　五十嵐　樹彦

平成２１（２００９）年　４月

目　　次

I．　総括研究報告
エイズ多剤併用療法中のリザーバーの特定および選択的障害に関する研究 ———— 3
五十嵐 樹彦

II.　研究成果の刊行に関する一覧表 ———————————————————————8

III.　研究成果の刊行物・別刷 ———————————————————————10

I. 厚生労働科学研究費補助金（エイズ対策研究事業）
（総括・分担）研究報告書

エイズ多剤併用療法中のリザーバーの特定および選択的障害に関する研究

研究代表者　五十嵐　樹彦　京都大学ウイルス研究所教授

研究要旨

サルエイズモデルを用いて多剤併用療法中もウイルスを保持し続けるリザーバーを同定する目的で、今年度はこのモデル系において確立されていない強力な抗ウイルス多剤療法の確立に取り組んだ。核酸系逆転写酵素阻害剤３剤及びプロテアーゼ阻害剤２剤、計５剤を経口で安定的に長期間投与できる方法を確立した。この方法で薬剤を投与したサルの血漿中薬剤濃度のトラフ値は感染者で推奨されている濃度を上回った。SIV 感染サルにこの多剤併用療法を適用すると、血漿中ウイルス量は投与開始後４週間以内に検出限界以下に抑制され、投与期間中維持された。HIV および SIV の主要な標的細胞であるメモリーCD4T 細胞が分布する肺実質では急性感染期に著減した同細胞の回復が多剤併用療法により加速された。しかし、化学療法中断後血漿中ウイルス量は速やかに上昇し、肺実質中の CD4T 細胞は減少した。以上の結果から、サルエイズモデルを用いて多剤併用療法中のリザーバーを検索する為の基盤整備が出来たと結論する。

A. 研究目的

抗 HIV-1 多剤併用療法の確立により、HIV-1 感染症は死に至る病ではなくなったが、この療法は未だ完全なものではなく、問題も認識されている。多剤併用療法の根本的な問題は感染者からウイルスを完全に排除する事が出来ない点であり、この為、感染者は薬剤を一生服用せねばならず、薬剤の副作用、変異ウイルスの出現、高額な医療費等の問題が派生する。本研究計画では多剤併用療法中にウイルスを保持し続けるリザーバーを特定、そのリザーバーを選択的に傷害する方法の開発を最終目的とする。リザーバーの全身レベルでの検索を行う為、サルエイズモデルである SIVmac/アカゲザル実験系を用いることとした。現在までこの実験系においてリザーバーの検索に応用できる様な強力な化学療法が存在しないので、今年度は SIVmac/アカゲザル実験系における多剤併用療法の確立を目標として薬剤の選択および投与方法を検討した。

B. 研究方法

多剤併用療法に用いる抗ウイルス薬として、抗 SIV 効果が知られている逆転写阻害剤ジドブジン(AZT)、ラミブジン（3TC)、テノフォビ

ル（TDF）を選択した。プロテアーゼ阻害剤は抗 SIV 効果が公表されているものが少ないため、入手可能な代表的な３剤、サキナビル(SQV)、ロピナビル(LPV)、アタザナビル（ATV）に関して、ヒトT細胞系株化細胞MT-4を用い、ウイルス感染による細胞死の阻止試験により抗 SIV 効果を検索した。投薬は選択した抗ウイルス剤（市販、成人感染者推奨服薬量の半量）を粉砕、同じく粉砕したサル飼料（PMI 社製 Certified animal diet 5048）30 グラムとバナナ 75 グラムを混合、成形し、１日２回(TDF のみ１日１回)、10 時間および 14 時間間隔で自由摂食させた。ウイルスは病原性 SIVmac239 を 2000TCID50 静脈内接種した。サルは中国産アカゲザル３頭を用い、１頭は非治療対照とし、２頭に多剤併用療法を感染 8 週後から 10 週間適用した。ウイルス接種前から経時的に末梢血および肺胞洗浄液中のリンパ球サブセットを解析した。ウイルス接種後、血漿中ウイルス RNA 量を PCR により経時的に定量した。

（倫理面への配慮）

実験は「研究機関等における動物実験等の実施に関する基本指針」に基づく「京都大学における動物実験の実施に関する規定」を遵守し行った。

C. 研究結果

検索したプロテアーゼ阻害剤三剤はそれぞれ異なる EC_{50} で SIV の複製を抑制した（SQV, 12.6nM, LPV, 38.6nM, ATV, 59.3nM)。同じ実験で HIV-1 と SIV を比較すると、SQV は SIV を、ATV は HIV-1 をより低濃度で、LPV はどちらもほぼ同じ濃度で抑制した。EC_{50} とヒトにおいて既に知られているそれぞれの薬剤の血中半減期を勘案し、LPV/リトナビルを選択した。

薬剤入り飼料を通常の飼料と置換したため、実験に用いた２頭のサルは投薬後１週間以内に摂食率が 90%に達し、その後安定して摂食した。投薬 14 時間後の薬物血中濃度を測定した所、10μM 以上であった。感染者が服用する際目標とされるトラフ値は 1-1.5μM であることから、投薬量は十分と判断した。

SIV 感染サルの血中ウイルス量は HAART を開始した接種８週後は 10^5 RNA コピー/ml だった。投薬開始後４週間以内に治療群２頭でウイルス量は検出限界の 200 RNA コピー/ml 以下に低下、治療期間中２回、数百コピー/ml の「ブリップ」を経験したがそれ以外は検出限界以下だった。

末梢血中の CD4 陽性リンパ球は治療の有無に関わらず大きな変動はなかったが、肺胞洗浄液中の CD4 陽性リンパ球はウイルス接種後４週以内に 45%から 5%程度に著減し、その後漸増した。この細胞は治療群２頭で治療期間中にウイルス接種前のレベルに戻ったが、非治療のサルでは接種前の 70%程度に留まった。

接種 18 週後に投薬を中断した所、治療群の血中ウイルス量は２週間以内に非治療サルと同じレベルになり、回復した肺胞洗浄液中の CD4 陽性リンパ球は投薬中止３週後から減少した。

D. 考察

以下の理由から今年度目標としたサルエイズモデルにおける多剤併用療法を確立したと考える。1）サルに安定して投薬可能である、2）感染者と同レベルの血中ウイルス量を4週間以内に検出限界以下に抑制した、3）投薬中は血中ウイルス量を安定して検出限界以下に抑制した。また、今回の結果から SIV 感染においても多剤併用療法の中止によって血中ウイルス量が速やかに上昇し、一端回復した CD4 陽性リンパ球が再び減少する事が確認された事から、療法中のリザーバーの検索に SIV/アカゲザルモデルが利用可能と考えられた。投薬量が多すぎる可能性は否めないが、10 週間の投薬後の血清生化学検査ではテノフォビルによる副作用として報告のある腎機能の異常を示唆するような数値は確認されなかった。治療中に観察された「ブリップ」に関してはインテグラーゼ阻害剤のような作用点の異なる抗ウイルス剤を更に加える事も考えられるが、多剤併用療法が成功している感染者でも見られる現象であるので、当面、今年度確立した療法を用いてリザーバーの検索に進みたい。

E. 結論

HIV-1 感染者に対して行われているのと同等のウイルス抑制効果のある多剤併用療法をサルエイズモデルにおいて確立した。

F. 健康危険情報

なし

G. 研究発表

1. 論文発表

- Fukazawa Y., Miyake A., Ibuki K., Inaba K., Saito N., Motohara M., Horiuchi R., Himeno A., Matsuda K., Matsuyama M., Takahashi H., Hayami M., Igarashi T., and Miura T. Small intestinal CD4+ T-cells are profoundly depleted during acute infection of simian-human immunodeficiency virus regardless of its pathogenicity. J.Virol. 82: 6039-6044, 2008.
- Laird, M.E., Igarashi, T., Martin, M.A., and Desrosiers, R.C. The importance of the V1/V2 loop region of simian-human immunodeficiency virus envelope gp120 in determining the strain specificity of the neutralizing antibody response. J.Virol. 82: 11054-11065, 2008.
- Morita, D., Katoh, K., Harada, T., Nakagawa, Y., Matsunaga, I., Miura, T., Adachi, A., Igarashi, T., and Sugita, M. Trans-species activation of human T cells by rhesus macaque CD1b molecules. Biochem.Biophys.Res.Commun. 377: 889-893, 2008.

2.学会発表

- Igarashi T.: "Work In Progress" toward developing a better non-human primate model for AIDS.9th Kumomoto AIDS Seminar, Sep.18-19, 2008, Kumamoto

- Inaba, K., Fukazawa, Y., Horiuchi, R., Matsuda, K., Himeno, A., Matsuyama, M., Hayami, M., Igarashi, T., Miura, T.: CD4+ cell reduction and enteropathy in small intestine can be occurred irrespective of viral load in simian/human immunodeficiency virus infection. 9th Kumomoto AIDS Seminar, Sep.18-19, 2008, Kumamoto

- Fukazawa, Y., Ibuki, K., Inaba, K., Saito, N., Matsuda, K., Himeno, A., Hirai, K., Matsuyama, M., Hayami, M., Igarashi, T., Miura, T.: Live attenuated AIDS vaccine conferred a strong protection against highly pathogenic SHIV challenge. 9th Kumomoto AIDS Seminar, Sep.18-19, 2008, Kumamoto

- Matsuda, K., Inaba, K., Ibuki, K., Fukazawa, Y., Matsuyama, M., Saito, N., Horiike, M., Hirai, K., Hayami, M., Igarashi, T., Miura, T.: Construction and in vivo analysis of R5 tropic SHIV. 9th Kumomoto AIDS Seminar, Sep.18-19, 2008, Kumamoto

- 稲葉一寿、深澤嘉伯、堀内励生、松田健太、姫野愛、松山めぐみ、伊吹謙太郎、速水正憲、五十嵐樹彦、三浦智行：SHIV-KS661長期感染アカゲザルにおけるウイルス増殖、CD4陽性T細胞の減少およびEnteropathyについて、第56回日本ウイルス学会学術集会、2008年10月26-28日、岡山

- 五十嵐樹彦：サルモデルを用いたHIV-1病原性の研究、シンポジウム4ヒトはなぜエイズになるのか、第22回日本エイズ学会学術集会、2008年11月26-28日、大阪

- 深澤嘉伯、伊吹謙太郎、稲葉一寿、齋藤尚紀、姫野愛、平井郁、松田健太、松山めぐみ、元原麻貴子、速水正憲、五十嵐樹彦、三浦智行：*nef*欠損弱毒生ワクチン免疫ザルに対する急性発症型SHIV攻撃接種後早期でのウイルス動態および免疫細胞の解析、第22回日本エイズ学会学術集会、2008年11月26-28日、大阪

- 松田健太、稲葉一寿、伊吹謙太郎、深澤嘉伯、松山めぐみ、斉藤尚紀、堀池麻里子、平井郁、姫野愛、速水正憲、五十嵐樹彦、三浦智行：ワクチン評価に有用なR5指向性SHIVの作製、第22回日本エイズ学会学術集会、2008年11月26-28日、大阪

- 堀池麻里子、松山めぐみ、佐藤彰彦、稲葉一寿、深澤嘉伯、松田健太、三浦智行、五十嵐樹彦：サル/エイズモデルにおけるHAART療法の確立に向けて、第22回日本エイズ学会学術集会、2008年11月26-28日、大阪

H. 知的財産権の出願・登録状況（予定を含む）

なし

II. 研究成果の刊行に関する一覧表

書籍　なし

雑誌

発表者氏名	論文タイトル名	発表誌名	巻号	ページ	出版年
Fukazawa Y., Miyake A., Ibuki K., Inaba K., Saito N., Motohara M., Horiuchi R., Himeno A., Matsuda K., Matsuyama M., Takahashi H., Hayami M., Igarashi T., Miura T.	Small intestinal $CD4^+$ T-cells are profoundly depleted during acute infection of simian-human immunodeficiency virus regardless of its pathogenicity.	The Journal of Virology	82	6039-6044	2008
Laird, M.E., Igarashi, T., Martin, M.A., Desrosiers, R.C.	The importance of the V1/V2 loop region of simian-human immunodeficiency virus envelope gp120 in determining the strain specificity of the neutralizing antibody response.	The Journal of Virology	82	11054-11065	2008
Morita, D., Katoh, K.,	Trans-species activation of human T cells by rhesus	Biochemical and Biophysical	377	889-893	2008

Harada, T., Nakagawa, Y., Matsunaga, I., Miura, T., Adachi, A., Igarashi, T., Sugita, M.	macaque CD1b molecules.	Research Communications			

III. 研究成果の刊行物・別刷

JOURNAL OF VIROLOGY, June 2008, p. 6039–6044 Vol. 82, No. 12
0022-538X/08/$08.00+0 doi:10.1128/JVI.02753-07

Small Intestine CD4$^+$ T Cells Are Profoundly Depleted during Acute Simian-Human Immunodeficiency Virus Infection, Regardless of Viral Pathogenicity$^\nabla$

Yoshinori Fukazawa,[1]† Ariko Miyake,[1,2]† Kentaro Ibuki,[1] Katsuhisa Inaba,[1] Naoki Saito,[1] Makiko Motohara,[1] Reii Horiuchi,[1] Ai Himeno,[1] Kenta Matsuda,[1] Megumi Matsuyama,[1] Hidemi Takahashi,[3] Masanori Hayami,[1] Tatsuhiko Igarashi,[1] and Tomoyuki Miura[1]*

Laboratory of Primate Model, Experimental Research Center for Infectious Diseases, Institute for Virus Research, Kyoto University, 53 Shogoinkawaramachi, Sakyo-ku, Kyoto 606-8507, Japan[1]; Laboratory of Tumor Cell Biology, Department of Medical Genome Sciences, Graduate School of Frontier Sciences, The University of Tokyo, Tokyo 162-8640, Japan[2]; and Department of Microbiology and Immunology, Nippon Medical School, Tokyo 113-8602, Japan[3]

Received 27 December 2007/Accepted 27 March 2008

To analyze the relationship between acute virus-induced injury and the subsequent disease phenotype, we compared the virus replication and CD4$^+$ T-cell profiles for monkeys infected with isogenic highly pathogenic (KS661) and moderately pathogenic (#64) simian-human immunodeficiency viruses (SHIVs). Intrarectal infusion of SHIV-KS661 resulted in rapid, systemic, and massive virus replication, while SHIV-#64 replicated more slowly and reached lower titers. Whereas KS661 systemically depleted CD4$^+$ T cells, #64 caused significant CD4$^+$ T-cell depletion only in the small intestine. We conclude that SHIV, regardless of pathogenicity, can cause injury to the small intestine and leads to CD4$^+$ T-cell depletion in infected animals during acute infection.

The highly pathogenic simian-human immunodeficiency virus (SHIV) SHIV-C2/1-KS661 (KS661), which was derived from SHIV-89.6 (23), replicates to high titers and causes the irreversible depletion of the circulating CD4$^+$ T cells during the acute phase of intravenous infection, followed by AIDS-like disease within 1 year (23). We previously reported that KS661 massively replicates and depletes CD4$^+$ T cells in both peripheral and mucosal lymphoid tissues during the initial 4 weeks postinfection (16). On the other hand, the isogenic SHIV-#64 (#64), which was derived from SHIV-89.6P, is moderately pathogenic. The genomic sequences of the two SHIVs differ by only 0.16%, resulting in a total of six amino acid changes in the products of the *pol*, *env-gp41*, and *rev* genes. The intravenous inoculation of rhesus macaques with #64 induces plasma viral burdens comparable to those induced by KS661 during the acute phase of infection and causes a transient reduction of the circulating CD4$^+$ T lymphocytes (10). After the acute phase, the viral loads decline to undetectable levels and the populations of CD4$^+$ T cells recover to preinfection levels.

To clarify the relationship between acute viral replication kinetics and subsequent clinical courses for these isogenic SHIVs with distinct pathogenicities, we examined proviral DNA, infectious-virus-producing cells (IVPCs), and CD4$^+$ T-cell depletion in peripheral and mucosal lymphoid tissues of 17 infected (Table 1) and 7 uninfected adult rhesus macaques (*Macaca mulatta*). Both Chinese and Indian rhesus monkeys were randomly assigned to these groups. The monkeys were used in accordance with the institutional regulations approved by the Committee for Experimental Use of Nonhuman Primates of the Institute for Virus Research, Kyoto University, Kyoto, Japan. The animals were inoculated via intrarectal infusion as described previously (17). Following serial euthanasia, tissues were collected and analyzed up to 27 days postinfection (dpi) as described previously (16, 17).

Gross virus replication was assessed by measuring plasma viral loads by reverse transcriptase PCR (16). By 6 dpi, plasma viral RNA levels became detectable in all the KS661-infected macaques (Fig. 1A) and three of seven #64-infected macaques (animals MM372, MM391, and MM374) (Fig. 1B). Although the plasma viral loads of the two groups at 13 dpi, when the virus loads reached their initial peaks, were not significantly different ($P = 0.1673$), the average load ($\pm$ the standard deviation) in KS661-infected monkeys ($9.3 \times 10^8 \pm 15.9 \times 10^8$ copies/ml) was about 10 times higher than that in #64-infected monkeys ($6.3 \times 10^7 \pm 11.6 \times 10^7$ copies/ml). These results suggest that KS661 spread faster and reached a somewhat higher titer than did #64 when the viruses were inoculated intrarectally.

Levels of peripheral blood CD4$^+$ T lymphocytes in all the KS661-infected monkeys decreased substantially within 4 weeks (Fig. 1C). On the other hand, the reductions in the levels of CD4$^+$ T cells varied among the #64-infected monkeys (Fig. 1D). For example, MM378 did not exhibit any appreciable changes, even though the plasma viral RNA load in this monkey reached 2.6×10^7 copies/ml by 21 dpi (Fig. 1 B and D).

* Corresponding author. Mailing address: Laboratory of Primate Model, Experimental Research Center for Infectious Diseases, Institute for Virus Research, Kyoto University, 53 Shogoinkawaramachi, Sakyo-ku, Kyoto 606-8507, Japan. Phone: 81-75-751-3984. Fax: 81-75-761-9335. E-mail: tmiura@virus.kyoto-u.ac.jp.
† These authors contributed equally to this work.
$^\nabla$ Published ahead of print on 9 April 2007.

TABLE 1. Experimental schedule for individual monkeys[a]

Virus (inoculum size)	Monkeys examined at:		
	6 dpi	13 dpi	27 dpi
KS661 (2×10^3 $TCID_{50}$)	MM300, MM309	MM313, MM334, MM392, MM393	MM308, MM310, MM394, MM395
#64 (2×10^5 $TCID_{50}$)	MM379, MM390	MM372, MM373*, MM391	MM374, MM378

[a] $TCID_{50}$, 50% tissue culture infective doses; *, MM373 received 2×10^3 $TCID_{50}$ of #64.

These data suggest that the decline in circulating $CD4^+$ T cells in KS661-infected animals was more severe and more reproducible than that in the #64-infected monkeys.

Another highly pathogenic SHIV, SHIV-DH12R, is known to cause systemic and synchronous replication events in animals following intravenous inoculation (6). To reveal the spread of virus in monkeys following intrarectal infection, we measured proviral DNA loads in a variety of tissues as described previously (16). KS661 proviral DNA was detected not only in samples from the rectums, the site of virus inoculation, but also in peripheral blood mononuclear cells and some lymph nodes (LN) at 6 dpi (Fig. 2A), suggesting that the virus was already spreading systemically. At 13 dpi, when the viral RNA loads in peripheral blood increased to the highest titers, proviral DNA levels in all of the tissues examined also increased, with levels in most monkeys exceeding 10^4 copies/μg of DNA. The levels of proviral DNA in all the tissues declined remarkably by 27 dpi. In contrast, #64 proviral DNA was detected only in the rectum of one (MM390) of the two monkeys examined at 6 dpi (Fig. 2A). At 13 dpi, the amount of proviral DNA in each tissue sample from #64-infected monkeys ($<10^4$ copies/μg of DNA) was considerably smaller than

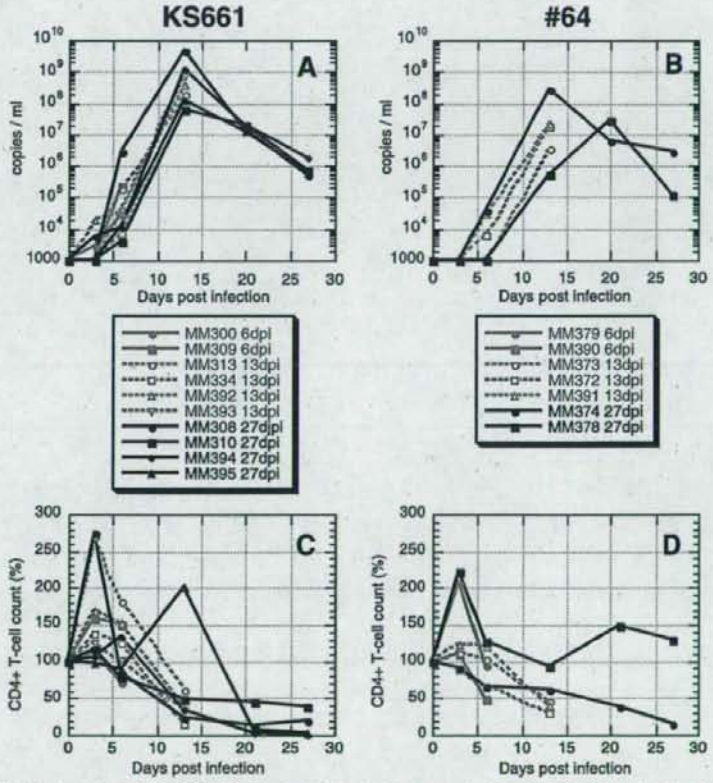

FIG. 1. Plasma viral RNA loads and profiles of circulating $CD4^+$ T cells for monkeys intrarectally infected with highly pathogenic KS661 and moderately pathogenic #64. (A and B) Plasma viral RNA loads were measured by quantitative reverse transcriptase PCR. The detection limit of this assay was 10^3 copies/ml. (C and D) Levels of $CD4^+$ T cells in peripheral blood samples from monkeys infected with KS661 and #64. The absolute number of $CD3^+$ $CD4^+$ cells in peripheral blood immediately before infection (day 0 postinfection) was defined as 100% for each monkey.

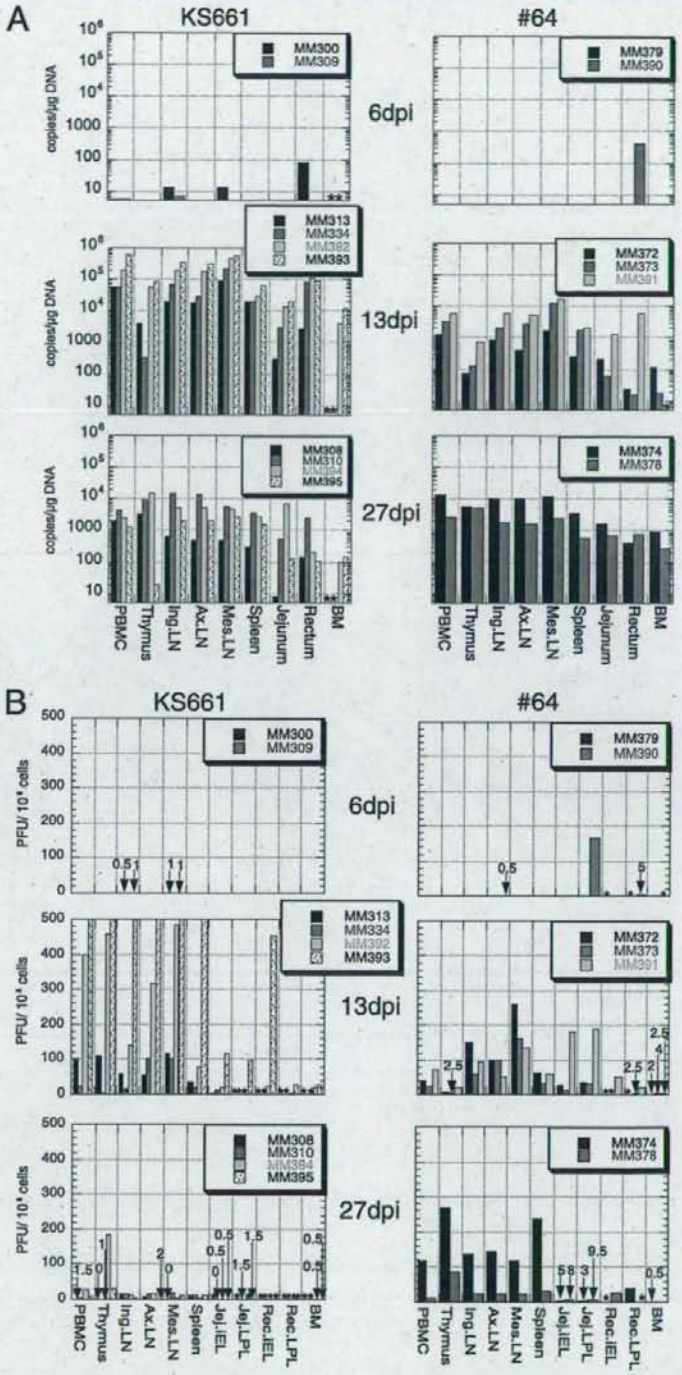

FIG. 2. (A) Proviral DNA loads in tissues of KS661- and #64-infected monkeys at 6, 13, and 27 dpi. Viral burdens were determined by quantitative PCR and expressed as the numbers of viral DNA copies per microgram of total DNA extracted from tissue homogenates. PBMC, peripheral blood mononuclear cells; Ing., inguinal; Ax., axillary; Mes., mesenteric; BM, bone marrow; *, not done. (B) Numbers of IVPCs in tissues of KS661- and #64-infected monkeys at 6, 13, and 27 dpi. Numbers of IVPCs were determined by an infectious plaque assay and were expressed as the numbers of PFU per 10^6 cells. Jej., jejunum; Rec., rectum; iEL, intraepithelial lymphocytes; *, not done.

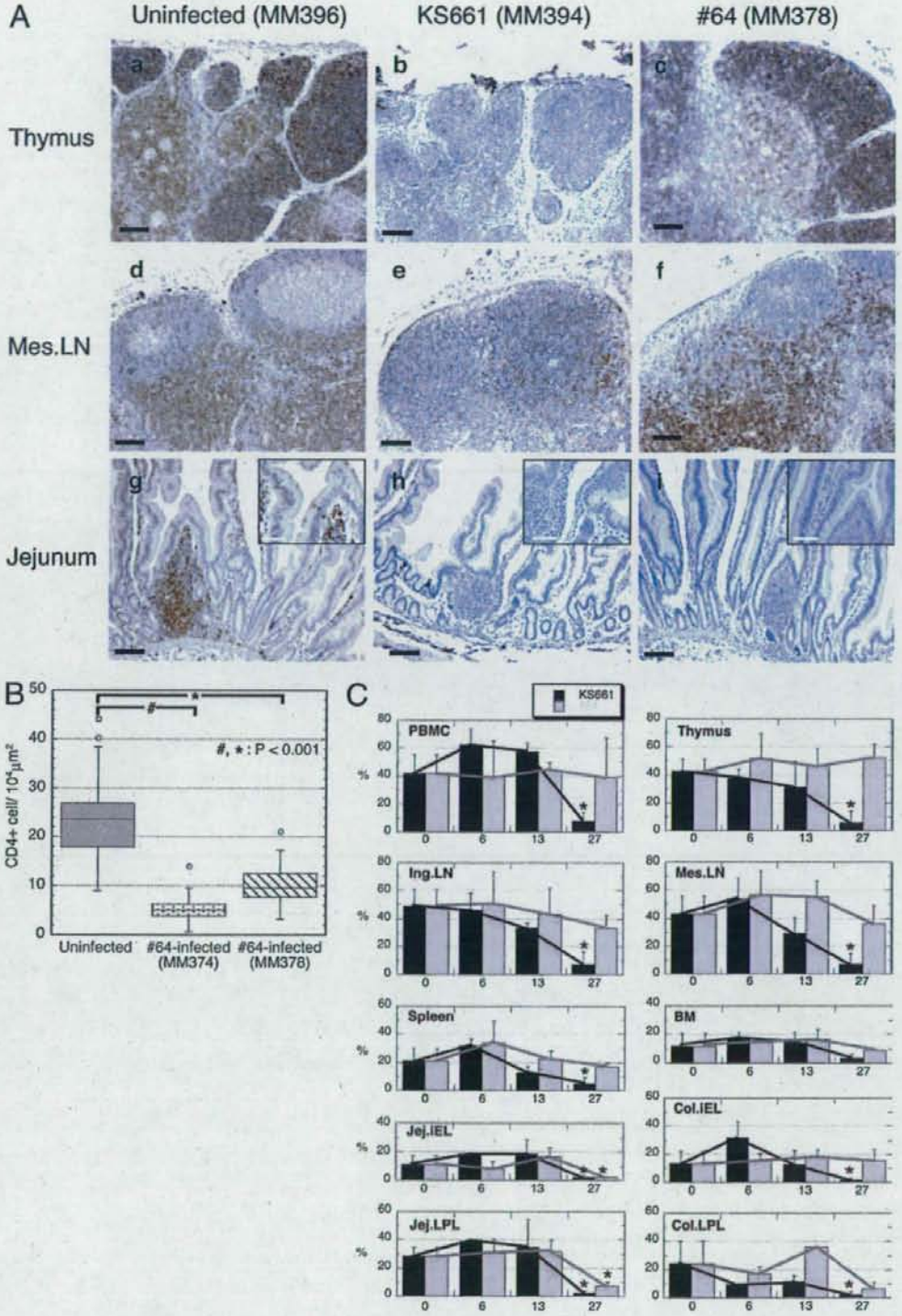

that in each sample from the KS661-infected monkeys. However, unlike the KS661 proviral DNA levels, the #64 proviral DNA levels in most tissues were maintained up to 27 dpi. These results suggest that #64 spread more slowly than KS661 and that the amounts of proviral DNA in a variety of tissues from the #64-infected animals were smaller than those in the tissues from KS661-infected animals around the initial peak of plasma viremia.

Because the amount of proviral DNA measured by PCR may include nonreplicating remnants of the viral genome, we also measured the number of IVPCs in each tissue sample by a plaque assay as described previously (9, 15). Briefly, cells prepared from infected animals were mixed with human T-lymphoid M8166 indicator cells, resuspended in culture medium containing 0.4% agarose, and plated into petri dishes. The plaques that formed in the cell layer were counted after 10 days of cultivation, and the number of IVPCs was calculated. For the KS661-infected monkeys, high numbers of IVPCs in all the tissue samples examined at 13 dpi were detected (Fig. 2B). Among these samples, the thymus and mesenteric LN samples harbored especially high numbers of IVPCs (more than 500/10^6 cells) at 13 dpi. The numbers of IVPCs declined remarkably from 13 to 27 dpi. We concluded that KS661 replicated systemically and synchronously in a variety of tissues, including the intestinal tract, at 13 dpi. In contrast, #64 production patterns in different tissues were not synchronous. Among #64-infected monkeys at 6 dpi, virus production was most active in the jejunum lamina propria lymphocytes (LPL) of MM390 (166 IVPCs/10^6 cells). At 13 dpi, interestingly, mesenteric LN became the center of virus production in two of the three monkeys examined (MM372 and MM373; 259 and 160 IVPCs/10^6 cells). In the other monkey (MM391), the jejunum had the highest number of IVPCs, followed by the mesenteric LN. These results suggested that the virus that replicated in the jejunum spread directly into the mesenteric LN via the flow of lymphatic fluid. At 27 dpi, the thymus tissues of both monkeys examined (MM374 and MM378) exhibited the highest numbers of IVPCs. In summary, the systemic dissemination of #64 was slower than that of KS661, and it was particularly delayed in the thymus during the acute phase.

Systemic $CD4^+$ cell depletion is the signature of disease induced by highly pathogenic SHIVs (7, 8, 22). We therefore compared the frequencies of $CD4^+$ cells in tissues from the animals infected with KS661 and #64, in addition to those of the circulating $CD4^+$ T lymphocytes. As representatives of the major virus-producing organs, the thymus, the mesenteric LN, and the jejunum were selected for examination. CD4 cell numbers were measured by immunohistochemistry analyses as described previously (18). Uninfected thymus tissue contained abundant $CD4^+$ cells that were stained brown (Fig. 3A, panel a), while the tissue collected from the KS661-infected animal at 27 dpi harbored few such cells (Fig. 3A, panel b). #64 caused virtually no $CD4^+$ cell depletion in the thymus at 27 dpi (Fig. 3A, panel c). In the mesenteric LN of uninfected monkeys, $CD4^+$ cells were found in the paracortical region (Fig. 3A, panel d). KS661 depleted $CD4^+$ cells in this area (Fig. 3A, panel e). Unlike KS661, #64 did not reduce the level of $CD4^+$ cells (Fig. 3A, panel f). The jejunum samples from uninfected animals contained $CD4^+$ cells in the lamina propria and follicles of gut-associated lymphatic tissues (Fig. 3 A, panel g). KS661 depleted $CD4^+$ cells in these tissues, too (Fig. 3A, panel h). Interestingly, #64 caused $CD4^+$ cell depletion in the small intestine comparable to that caused by KS661 (Fig. 3A, panel i). To confirm the observed cell reduction in the jejunum samples, we randomly selected a total of 40 fields on the tissue sections from each animal for viewing at a total magnification of ×400, counted $CD4^+$ cells, and averaged the numbers (Fig. 3B). The $CD4^+$ cell densities in the jejunum samples from the #64-infected monkeys were significantly lower than those in the samples from uninfected animals ($P < 0.001$). This gut-specific $CD4^+$ cell depletion caused by #64 prompted us to analyze the frequencies of $CD4^+$ T cells (including CD4 and CD8 doubly positive cells) in a variety of tissues by flow cytometry (Fig. 3C). KS661 caused systemic $CD4^+$ T-lymphocyte depletion by 27 dpi (Fig. 3C). In agreement with the immunohistochemistry results, #64 significantly depleted $CD4^+$ T cells only in the jejunum intraepithelial lymphocytes and LPL ($P = 0.01$ and 0.003, respectively) (Fig. 3C) by 27 dpi, although we examined only two #64-infected monkeys at 27 dpi. In conclusion, the $CD4^+$ T-cell depletion patterns caused by KS661 and #64 were distinct, and the small intestine was the only site in which $CD4^+$ T cells were significantly depleted by the moderately pathogenic #64.

Taken together, our results show that #64 disseminated more slowly and replicated less than KS661 in systemic lymphoid tissues, as well as in peripheral blood, during the acute phase of infection. We believe that because of its low rate and low levels of replication, #64 could not cause irreversible injury before the host mounted an immune reaction. As a result, $CD4^+$ T cells were not completely depleted in all the tissues examined, except in the small intestine. These results suggest that the small intestine is the tissue most sensitive to virus-induced $CD4^+$ T-cell depletion during the acute phase of infection. Recent reports revealed that severe acute depletions

FIG. 3. Profiles of $CD4^+$ T cells in systemic lymphoid tissues during acute infection. (A) Immunohistochemical staining for CD4 molecules (stained brown) in the thymus, mesenteric (mes.) LN, and jejunum tissues of KS661- or #64-infected monkeys at 27 dpi, in addition to those of uninfected monkeys. Black scale bars, 100 μm; white scale bars in insets of panels g, h, and i, 50 μm. (B) Comparison of $CD4^+$ cell frequencies in the jejunum LPL of uninfected and #64-infected monkeys at 27 dpi. A total of forty randomly selected fields (total magnification, ×400) of at least four tissue sections per animal were used for the analysis of jejunum LPL. *P* values (determined by Student's *t* test with 95% confidence intervals) are for comparisons of each #64-infected monkey with uninfected monkeys. (C) Percentages of $CD4^+$ T cells among total lymphocytes from KS661- and #64-infected monkeys. In each graph, data for 0 dpi (time points postinfection are shown along the *x* axis) are averages of percentages for seven uninfected control monkeys. Percentages of $CD4^+$ T cells (including CD4 and CD8 doubly positive cells) were obtained by first gating lymphocytes and then $CD3^+$ T cells with a flow cytometer. PBMC, peripheral blood mononuclear cells; Ing., inguinal; Jej., jejunum; iEL, intraepithelial lymphocytes; BM, bone marrow; Col., colon; *, $P < 0.05$ (percentage at 0 dpi versus that at 27 dpi; Student's *t* test with a 95% confidence interval).

of mucosal CD4$^+$ T cells have been observed in simian immunodeficiency virus-infected monkeys (11, 12, 24, 25) and human immunodeficiency virus-infected humans (2, 5, 13). The acute depletion of mucosal CD4$^+$ T cells and the disease outcome are correlated (1, 3, 21, 26). However, a decrease of mucosal CD4$^+$ T cells has also been observed in the early phases of natural host infections, such as SIVagm infection in African green monkeys and SIVsmm infection in sooty mangabeys, which typically do not progress to AIDS (4, 14, 19). In addition, the levels of apoptosis and immune activation and the degrees of CD4$^+$ T-cell restoration differ between progressors and nonprogressors in simian immunodeficiency virus models (4, 14, 19). Taken together, these results raise the possibility that the severe acute depletion of mucosal CD4$^+$ T cells is not sufficient to induce AIDS. The restoration of CD4$^+$ T cells and normal immune function after the severe acute depletion may define the eventual disease outcome (20). The abilities of KS661- and #64-infected monkeys to restore the immune system may be different, because KS661, but not #64, impairs thymic T-cell differentiation (18). Currently, we are focusing on the restoration of CD4$^+$ T cells and the functional aspect of the immune cells in the small intestines of animals infected with KS661 and #64 to further clarify the determinant(s) of the disease outcome.

We are grateful to James Raymond for English editing of the manuscript and to Takahito Kazama for technical support.

This work was supported, in part, by Research on Human Immunodeficiency Virus/AIDS in Health and Labor Sciences research grants from the Ministry of Health, Labor and Welfare, Japan, a grant-in-aid for scientific research from the Ministry of Education and Science, Japan, a research grant for health sciences focusing on drug innovation for AIDS from the Japan Health Sciences Foundation, and a grant from the Program for the Promotion of Fundamental Studies in Health Sciences of the National Institute of Biomedical Innovation (NIBIO) of Japan.

REFERENCES

1. **Brenchley, J. M., D. A. Price, and D. C. Douek.** 2006. HIV disease: fallout from a mucosal catastrophe? Nat. Immunol. **7**:235–239.
2. **Brenchley, J. M., T. W. Schacker, L. E. Ruff, D. A. Price, J. H. Taylor, G. J. Beilman, P. L. Nguyen, A. Khoruts, M. Larson, A. T. Haase, and D. C. Douek.** 2004. CD4$^+$ T cell depletion during all stages of HIV disease occurs predominantly in the gastrointestinal tract. J. Exp. Med. **200**:749–759.
3. **Chase, A., Y. Zhou, and R. F. Siliciano.** 2006. HIV-1-induced depletion of CD4$^+$ T cells in the gut: mechanism and therapeutic implications. Trends Pharmacol. Sci. **27**:4–7.
4. **Gordon, S. N., N. R. Klatt, S. E. Bosinger, J. M. Brenchley, J. M. Milush, J. C. Engram, R. M. Dunham, M. Paiardini, S. Klucking, A. Danesh, E. A. Strobert, C. Apetrei, I. V. Pandrea, D. Kelvin, D. C. Douek, S. I. Staprans, D. L. Sodora, and G. Silvestri.** 2007. Severe depletion of mucosal CD4$^+$ T cells in AIDS-free simian immunodeficiency virus-infected sooty mangabeys. J. Immunol. **179**:3026–3034.
5. **Guadalupe, M., E. Reay, S. Sankaran, T. Prindiville, J. Flamm, A. McNeil, and S. Dandekar.** 2003. Severe CD4$^+$ T-cell depletion in gut lymphoid tissue during primary human immunodeficiency virus type 1 infection and substantial delay in restoration following highly active antiretroviral therapy. J. Virol. **77**:11708–11717.
6. **Igarashi, T., C. R. Brown, R. A. Byrum, Y. Nishimura, Y. Endo, R. J. Plishka, C. Buckler, A. Buckler-White, G. Miller, V. M. Hirsch, and M. A. Martin.** 2002. Rapid and irreversible CD4$^+$ T-cell depletion induced by the highly pathogenic simian/human immunodeficiency virus SHIV(DH12R) is systemic and synchronous. J. Virol. **76**:379–391.
7. **Igarashi, T., Y. Endo, G. Englund, R. Sadjadpour, T. Matano, C. Buckler, A. Buckler-White, R. Plishka, T. Theodore, R. Shibata, and M. A. Martin.** 1999. Emergence of a highly pathogenic simian/human immunodeficiency virus in a rhesus macaque treated with anti-CD8 mAb during a primary infection with a nonpathogenic virus. Proc. Natl. Acad. Sci. USA **96**:14049–14054.
8. **Joag, S. V., Z. Li, L. Foresman, E. B. Stephens, L.-J. Zhao, I. Adany, D. M. Pinson, H. M. McClure, and O. Narayan.** 1996. Chimeric simian/human immunodeficiency virus that causes progressive loss of CD4$^+$ T cells and AIDS in pig-tailed macaques. J. Virol. **70**:3189–3197.
9. **Kato, S., Y. Hiraishi, N. Nishimura, T. Sugita, M. Tomihama, and T. Takano.** 1998. A plaque hybridization assay for quantifying and cloning infectious human immunodeficiency virus type 1 virions. J. Virol. Methods **72**:1–7.
10. **Kozyrev, I. L., K. Ibuki, T. Shimada, T. Kuwata, T. Takemura, M. Hayami, and T. Miura.** 2001. Characterization of less pathogenic infectious molecular clones derived from acute-pathogenic SHIV-89.6p stock virus. Virology **282**:6–13.
11. **Li, Q., L. Duan, J. D. Estes, Z. M. Ma, T. Rourke, Y. Wang, C. Reilly, J. Carlis, C. J. Miller, and A. T. Haase.** 2005. Peak SIV replication in resting memory CD4$^+$ T cells depletes gut lamina propria CD4$^+$ T cells. Nature **434**:1148–1152.
12. **Mattapallil, J. J., D. C. Douek, B. Hill, Y. Nishimura, M. Martin, and M. Roederer.** 2005. Massive infection and loss of memory CD4$^+$ T cells in multiple tissues during acute SIV infection. Nature **434**:1093–1097.
13. **Mehandru, S., M. A. Poles, K. Tenner-Racz, A. Horowitz, A. Hurley, C. Hogan, D. Boden, P. Racz, and M. Markowitz.** 2004. Primary HIV-1 infection is associated with preferential depletion of CD4$^+$ T lymphocytes from effector sites in the gastrointestinal tract. J. Exp. Med. **200**:761–770.
14. **Milush, J. M., J. D. Reeves, S. N. Gordon, D. Zhou, A. Muthukumar, D. A. Kosub, E. Chacko, L. D. Giavedoni, C. C. Ibegbu, K. S. Cole, J. L. Miamidian, M. Paiardini, A. P. Barry, S. I. Staprans, G. Silvestri, and D. L. Sodora.** 2007. Virally induced CD4$^+$ T cell depletion is not sufficient to induce AIDS in a natural host. J. Immunol. **179**:3047–3056.
15. **Miyake, A., Y. Enose, S. Ohkura, H. Suzuki, T. Kuwata, T. Shimada, S. Kato, O. Narayan, and M. Hayami.** 2004. The quantity and diversity of infectious viruses in various tissues of SHIV-infected monkeys at the early and AIDS stages. Arch. Virol. **149**:943–955.
16. **Miyake, A., K. Ibuki, Y. Enose, H. Suzuki, R. Horiuchi, M. Motohara, N. Saito, T. Nakasone, M. Honda, T. Watanabe, T. Miura, and M. Hayami.** 2006. Rapid dissemination of a pathogenic simian/human immunodeficiency virus to systemic organs and active replication in lymphoid tissues following intrarectal infection. J. Gen. Virol. **87**:1311–1320.
17. **Miyake, A., K. Ibuki, H. Suzuki, R. Horiuchi, N. Saito, M. Motohara, M. Hayami, and T. Miura.** 2005. Early virological events in various tissues of newborn monkeys after intrarectal infection with pathogenic simian human immunodeficiency virus. J. Med. Primatol. **34**:294–302.
18. **Motohara, M., K. Ibuki, A. Miyake, Y. Fukazawa, K. Inaba, H. Suzuki, K. Masuda, N. Minato, H. Kawamoto, T. Nakasone, M. Honda, M. Hayami, and T. Miura.** 2006. Impaired T-cell differentiation in the thymus at the early stages of acute pathogenic chimeric simian-human immunodeficiency virus (SHIV) infection in contrast to less pathogenic SHIV infection. Microbes Infect. **8**:1539–1549.
19. **Pandrea, I. V., R. Gautam, R. M. Ribeiro, J. M. Brenchley, I. F. Butler, M. Pattison, T. Rasmussen, P. A. Marx, G. Silvestri, A. A. Lackner, A. S. Perelson, D. C. Douek, R. S. Veazey, and C. Apetrei.** 2007. Acute loss of intestinal CD4$^+$ T cells is not predictive of simian immunodeficiency virus virulence. J. Immunol. **179**:3035–3046.
20. **Picker, L. J.** 2006. Immunopathogenesis of AIDS virus infection. Curr. Opin. Immunol. **18**:399–405.
21. **Picker, L. J., and D. I. Watkins.** 2005. HIV pathogenesis: the first cut is the deepest. Nat. Immunol. **6**:430–432.
22. **Reimann, K. A., J. T. Li, R. Veazey, M. Halloran, I. W. Park, G. B. Karlsson, J. Sodroski, and N. L. Letvin.** 1996. A chimeric simian/human immunodeficiency virus expressing a primary patient human immunodeficiency virus type 1 isolate *env* causes an AIDS-like disease after in vivo passage in rhesus monkeys. J. Virol. **70**:6922–6928.
23. **Shinohara, K., K. Sakai, S. Ando, Y. Ami, N. Yoshino, E. Takahashi, K. Someya, Y. Suzaki, T. Nakasone, Y. Sasaki, M. Kaizu, Y. Lu, and M. Honda.** 1999. A highly pathogenic simian/human immunodeficiency virus with genetic changes in cynomolgus monkey. J. Gen. Virol. **80**:1231–1240.
24. **Smit-McBride, Z., J. J. Mattapallil, M. McChesney, D. Ferrick, and S. Dandekar.** 1998. Gastrointestinal T lymphocytes retain high potential for cytokine responses but have severe CD4$^+$ T-cell depletion at all stages of simian immunodeficiency virus infection compared to peripheral lymphocytes. J. Virol. **72**:6646–6656.
25. **Veazey, R. S., M. DeMaria, L. V. Chalifoux, D. E. Shvetz, D. R. Pauley, H. L. Knight, M. Rosenzweig, R. P. Johnson, R. C. Desrosiers, and A. A. Lackner.** 1998. Gastrointestinal tract as a major site of CD4$^+$ T cell depletion and viral replication in SIV infection. Science **280**:427–431.
26. **Veazey, R. S., and A. A. Lackner.** 2004. Getting to the guts of HIV pathogenesis. J. Exp. Med. **200**:697–700.

JOURNAL OF VIROLOGY, Nov. 2008, p. 11054–11065 Vol. 82, No. 22
0022-538X/08/$08.00+0 doi:10.1128/JVI.01341-08

Importance of the V1/V2 Loop Region of Simian-Human Immunodeficiency Virus Envelope Glycoprotein gp120 in Determining the Strain Specificity of the Neutralizing Antibody Response[▽]

Melissa E. Laird,[1] Tatsuhiko Igarashi,[2] Malcolm A. Martin,[3] and Ronald C. Desrosiers[1]*

New England Primate Research Center, Department of Microbiology and Molecular Genetics, Harvard Medical School, Southborough, Massachusetts 01772-9102[1]; Laboratory of Primate Models, Experimental Research Center for Infectious Diseases, Institute for Virus Research, Kyoto University, Kyoto 606-8057, Japan[2]; and Laboratory of Molecular Microbiology, National Institute of Allergy and Infectious Diseases, National Institutes of Health, Bethesda, Maryland 20892[3]

Received 26 June 2008/Accepted 28 August 2008

Plasma samples from individuals infected with human immunodeficiency virus type 1 (HIV-1) are known to be highly strain specific in their ability to neutralize HIV-1 infectivity. Such plasma samples exhibit significant neutralizing activity against autologous HIV-1 isolates but typically exhibit little or no activity against heterologous strains, although some cross-neutralizing activity can develop late in infection. Monkeys infected with the simian-human immunodeficiency virus (SHIV) clone DH12 generated antibodies that neutralized SHIV DH12, but not SHIV KB9. Conversely, antibodies from monkeys infected with the SHIV clone KB9 neutralized SHIV KB9, but not SHIV DH12. To investigate the role of the variable loops of the HIV-1 envelope glycoprotein gp120 in determining this strain specificity, variable loops 1 and 2 (V1/V2), V3, or V4 were exchanged individually or in combination between SHIV DH12 and SHIV KB9. Despite the fact that both parental viruses exhibited significant infectivity and good replication in the cell lines examined, 3 of the 10 variable-loop chimeras exhibited such poor infectivity that they could not be used further for neutralization assays. These results indicate that a variable loop that is functional in the context of one particular envelope background will not necessarily function within another. The remaining seven replication-competent chimeras allowed unambiguous assignment of the sequences principally responsible for the strain specificity of the neutralizing activity present in SHIV-positive plasma. Exchange of the V1/V2 loop sequences conferred a dominant loss of sensitivity to neutralization by autologous plasma and a gain of sensitivity to neutralization by heterologous plasma. Substitution of V3 or V4 had little or no effect on the sensitivity to neutralization. These data demonstrate that the V1/V2 region of HIV-1 gp120 is principally responsible for the strain specificity of the neutralizing antibody response in monkeys infected with these prototypic SHIVs.

In order to achieve complete and durable protection against human immunodeficiency virus (HIV), it has been suggested that a vaccine may have to elicit a potent, broadly neutralizing antibody response as well as a strong cell-mediated immune response (93). Multiple studies have shown that passive transfer of HIV-specific antibodies is able to provide sterile protection against HIV type 1 (HIV-1) or simian-HIV (SHIV) challenge, whether administered intravenously or mucosally, in various animal models of infection (3, 32, 57, 58, 70, 73, 85). Moreover, several unusual, well-characterized monoclonal antibodies that are broadly acting, relatively potent, and capable of neutralizing viruses in a cross-clade manner have been isolated from HIV-infected individuals (7, 9, 13, 34, 78, 88, 91). These studies demonstrate that neutralizing antibodies can, at least in theory, provide protection against HIV-1 infection. However, envelope-based immunogens developed to date have not been capable of eliciting a robust antibody response with the broad target specificity and high plasma concentrations that are likely to be necessary for protection (5, 12, 20, 22, 24–26, 31, 56, 59, 62, 92).

HIV-1 infection in humans typically elicits high levels of antibodies directed against the viral surface glycoprotein gp120. It has been estimated that as much as 5% of all immunoglobulin in some HIV-infected individuals may be directed to the virus-encoded surface glycoprotein (6). However, the abilities of these antibodies to neutralize HIV-1 infectivity are extremely limited in both potency and breadth. The neutralizing antibodies that are elicited upon HIV-1 infection tend to be highly strain specific; they neutralize autologous virus most effectively but exhibit little or no neutralizing activity against heterologous HIV-1 strains (10, 11, 61, 74, 81). Due to rapid sequence evolution within the envelope protein in response to immune pressure and selection, the original antibody population loses potency over the course of infection as persistently replicating viruses acquire resistance to antibody-mediated detection. There is a responsive shift in the production of neutralizing antibodies over time, apparently evolving new target specificities to counter newly emerged viral variants (1, 29, 33, 81, 95).

The HIV-1 envelope glycoprotein is the primary target for

* Corresponding author. Mailing address: New England Primate Research Center, One Pine Hill Drive, Southborough, MA 01772-9102. Phone: (508) 624-8040. Fax: (508) 624-8190. E-mail: ronald_desrosiers@hms.harvard.edu.

▽ Published ahead of print on 3 September 2008.

antibody-mediated neutralization (2, 4). In order to circumvent antibody recognition, HIV-1 has evolved a number of shielding strategies to occlude conserved epitopes and limit the accessibility of glycoprotein spikes on the surfaces of virions to antibody binding. The mature envelope spike exists as a trimer of gp120-gp41 noncovalently associated heterodimers. Each trimer is tightly packed in a closed conformation such that epitopes that otherwise might serve as targets for antibody binding and neutralization reside in the core of the protein and are not readily exposed (45, 66, 67, 77). Additionally, gp120 contains five distinct regions that are characterized by extensive sequence variation. Four of these hypervariable regions are thought to form loops through intrachain disulfide bonds that are exposed on the outer surface of the envelope protein, resulting in the occlusion of conserved core envelope epitopes from antibody recognition prior to viral entry (38, 40, 50, 54, 96).

A number of studies have been performed to explore the roles of the variable loops as immunological decoys or in shielding conserved elements within the core of the envelope. Surprisingly, the deletion of the entire variable loop 1 and 2 (V1/V2) complex, as many as 100 amino acids, can still yield replication-competent HIV-1 or simian immunodeficiency virus (SIV) (44, 97). These V1/V2 deletion mutants are substantially more sensitive to neutralization by a panel of monoclonal antibodies targeting multiple epitopes on gp120 (14, 44, 46, 52, 83, 84, 87, 97). Several highly strain-specific neutralizing antibodies targeting the V1 and/or V2 loop have been identified, although exact epitopes have not yet been defined (18, 27, 28, 30, 89). A considerable body of evidence suggests that the majority of anti-V3 antibodies are also strain specific and can efficiently neutralize tissue culture-adapted virus strains but not primary isolates (65). In SIV infection, the V4 loop contains a conformational, neutralization-sensitive epitope in which sequence changes emerge to escape antibody detection (43, 90).

The present study examines the role of variable-loop sequences in the strain specificity of antibody-mediated neutralization. To investigate if certain variable loops might be responsible for the strain-specific neutralizing activity characteristic of HIV-1-positive plasma, we constructed a panel of chimeric viruses between SHIV DH12 and SHIV KB9, exchanging each variable loop between both SHIV envelopes individually and in combination. We then examined the effects of these variable-loop exchanges on virus infectivity and sensitivity to highly strain-specific plasma samples collected from SHIV DH12- and SHIV KB9-infected monkeys. Seven of the 10 SHIV-derived variable-loop chimeras were replication competent and capable of inducing robust secreted alkaline phosphatase (SEAP) production in the C8166-45 LTR-SEAP cell line. We demonstrate that the exchange of the V1/V2 loop complex between SHIV DH12 and SHIV KB9 is consistently associated with a dramatic loss of sensitivity to autologous plasma and a gain of sensitivity to heterologous plasma. Our results demonstrate that the V1/V2 loop is the principal determinant of the strain specificity of the neutralizing-antibody response in SHIV-infected monkeys.

MATERIALS AND METHODS

PCR mutagenesis and plasmid construction. Mutations within *env* were generated by a two-step PCR method that combined the technique of splicing by overlap extension PCR (69) to generate a primary product with site-directed PCR mutagenesis to incorporate the mutations into the hemigenomic plasmids. For SHIV KB9, initial mutagenesis was performed on the 3′ half of the genome, which was obtained from the NIH AIDS Research and Reference Reagent Program (Division of AIDS, National Institute of Allergy and Infectious Diseases, NIH) (47). The full-length proviral plasmid DNA of SHIV DH12 was kindly provided by T. Igarashi and M. A. Martin (86). To facilitate optimal mutagenesis efficiency for the SHIV DH12 envelope sequence, the envelope gene was subcloned from the full-length genome.

For the splicing by overlap extension step of our mutagenesis protocol, two overlapping PCR products were generated, with the desired substitution incorporated in the region of overlap. Specifically, the amplified and incorporated fragment was the complete variable-loop sequence under investigation. Each primer included, in its 5′ portion, nucleotides complementary to the backbone envelope sequence and, in its 3′ half, nucleotides complementary to the variable-loop sequence of interest. These primers were combined with the plasmid DNA containing the variable-loop sequence. The result was a pool of PCR products containing the amplified variable-loop sequence flanked by single-stranded overhangs of sequence complementary to the reciprocal envelope sequence. These purified variable-loop amplicons were used in lieu of primers for site-directed mutagenesis (Stratagene, La Jolla, CA) reactions using the envelope subclones as template DNA.

The following paired primers were used to generate the amplicons necessary for creating the variable-loop chimeric envelopes (the first capitalized letter indicates the SHIV envelope background, and the SHIV strain that is the source of the variable loop exchanged is indicated by the lowercase abbreviation prior to the variable-loop identification; within the primer sequence, the loop sequences that are being introduced are underlined): K.dV1V2F, 5′ CC CCA CTC TGT GTT ACT TTA AAT TGC ACT GAT TTG AAG AAT GG 3′; K.dV1V2R, 5′ GGC CTG TGT AAT GAC TGA GGT GTT ACA ACT TAT CAA CCT ATA GC 3′; K.dV3F, 5′ CAG CTA AAT GAA TCT GTA GTA ATT AAT TGT ACA AGA CCC AAC AAC AAT ACA AGA AAA GGG 3′; K.dV3R, 5′ CCA TTT TGC TCT ACT AAT GTT ACA ATG TGC TTG TCT TAT ATC TCC 3′; K.dV4F, 5′ GGA GGG GAA TTT TTC TAC TGT AAT ACA AAA AAA CTG 3′; K.dV4R, 5′ CC TAC TTT CTG CCA CAT ATT TAT AAT TTG TTT TAT TCT GCA TGG GAG TGT GAT AGT GTC ATT TCC 3′; D.kV1V2F, 5′ CC CCA CTC TGT GTT ACT TTA CAT TGC ACT AAT TTG AAT ATC AC 3′; D.kV1V2R, 5′ GG ACA GGC CTG TGT AAG GGT TGA GGT GTT ACA ACT TAT TAA CCT ATA CTT AG 3′; D.kV3F, 5′ CAG CTG AAT GAA ACT GTA GAA ATT AAT TGT ACA AGA CCC AAC AAC AAT ACA AGA GAA AGG 3′; D.kV3R, 5′ G CCA TTT TAC TTT ACT AAT GTT ACA ATG TGC TTG TCT TAT ATC TCC 3′; D.kV4F, 5′ GT GGA GGG GAA TTT TTC TAC TGT AAT ACA GCA CAA CTG TTT AAT AGT ACT TGG 3′; D.kV4R, 5′ C CTG CCA CAT GTT TAT AAT TTG TTT TAT TCT GCA TTG GAG TGT GAT TAT GTC ATT TCC 3′ (Sigma Genosys, The Woodlands, TX).

The variable-loop-exchanged envelopes within the envelope subclones were sequenced to verify accuracy. In the constructs that contained variable loops exchanged in combination, this process was repeated sequentially. Sequencing of these combinatorial constructs was performed subsequent to each mutagenesis step. Full-length proviral DNA clones of each mutant were constructed.

DNA sequencing. Cloned plasmids containing selected mutations were sequenced with a CEQ8000 genetic-analysis system, using a dye terminator cycle-sequencing chemistry kit as specified by the manufacturer (Beckman-Coulter, Fullerton, CA).

Virus stocks and cell culture. To generate virus stocks, 5 μg of the appropriate full-length proviral DNA plasmid was transfected into 1.5×10^6 HEK 293T cells using the calcium phosphate method (Promega, Madison, WI). The medium was changed 24 h posttransfection. Supernatants were harvested on day 3 posttransfection. Virus concentrations in the supernatant were quantified by determining the concentration of p27 capsid protein using an antigen capture assay, according to the manufacturer's instructions (Advanced Bioscience Laboratories, Inc., Kensington, MD). HEK 293T, MT4, C8166, and C8166-45 LTR-SEAP cells were cultured and maintained as described previously (10, 60).

Infectivity assay. Viral infectivity was quantified using the C8166-45 LTR-SEAP indicator cell line (60). C8166-45 LTR-SEAP cells contain a Tat-inducible SEAP reporter construct allowing SIV infection of the cells to be measured by SEAP concentrations in the cell-free supernatant. Nine serial twofold dilutions were made, starting from 10 ng of p27 capsid equivalents of HEK 293T cell-produced stocks. C8166-45 LTR-SEAP cells (8,000) were added to each

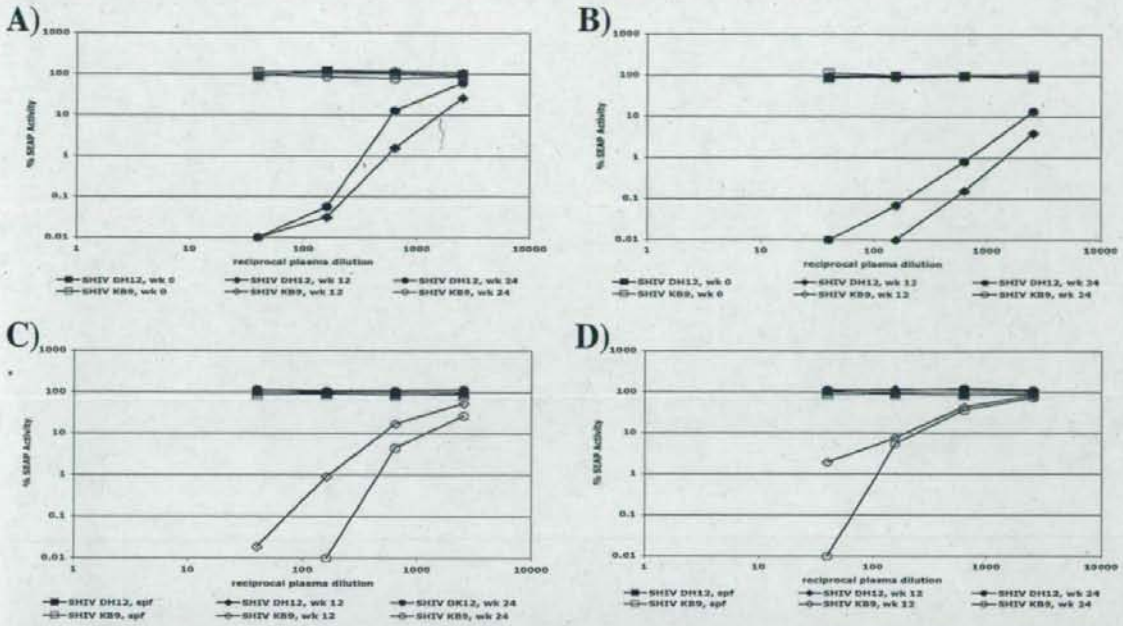

FIG. 1. Strain-specific neutralizing activity of positive plasmas when assayed with SHIV DH12 and SHIV KB9. (A) Neutralization of SHIV DH12 and SHIV KB9 with positive plasma from a SHIV DH12-infected monkey, RHTPP, collected at 0, 12, and 24 weeks (wk) postinfection. (B) Neutralization of SHIV DH12 and SHIV KB9 with positive plasma from a SHIV DH12-infected monkey, Rh418, collected at 0, 12, and 24 weeks postinfection. (C) Neutralization of SHIV DH12 and SHIV KB9 with positive plasma from a SHIV KB9-infected monkey, 477-99 collected 12 and 24 weeks postinfection, as well as with plasma from a SHIV-negative, specific-pathogen-free (SPF) monkey. (D) Neutralization of SHIV DH12 and SHIV KB9 with positive plasma from a SHIV KB9-infected monkey, 481-99, collected 12 and 24 weeks postinfection, as well as with plasma from an SPF monkey.

well. The cells were incubated at 37°C in a humidified CO_2 incubator. Three days postinfection, SEAP activity was measured in the cell-free supernatant (Applied Biosystems, Foster City, CA).

SHIV-positive plasmas. Five plasma samples taken at selected time points postinfection from rhesus macaques infected with SHIV DH12 were obtained from Malcolm Martin (National Institute of Allergy and Infectious Diseases, NIH, Bethesda, MD). Four plasma samples taken at selected time points postinfection from rhesus macaques infected with SHIV KB9 were available from a previous study performed at the New England Primate Research Center.

Neutralization. The neutralization sensitivity of each virus to both SHIV-positive monkey plasmas was assayed using the SEAP reporter cell assay as described previously (60). Virus equivalent to 2.5 ng of p27 capsid protein was determined to be the lowest level of virus input sufficient to give a reliable SEAP signal within the linear range of the assay for all of the virus strains used. SEAP activity was quantified on the earliest day postinfection when levels were sufficiently high over background to give consistent measurements (at least 10-fold), ranging from 3 days for SHIV DH12, SHIV KB9, SHIV KDV3, and SHIV KDV4 to 5 days for SHIV DKV12, SHIV DKV4, SHIV DKV1234, and SHIV KDV1234 and 7 days for SHIV DKV124.

To perform neutralization assays, 96-well plates were organized as follows. Twenty-five microliters of medium (RPMI 1640 supplemented with 10% fetal bovine serum, penicillin/streptomycin, L-glutamine, and HEPES buffer [R10]) was added to each well in the first three columns. To the wells in the remaining columns (columns 4 to 12), 25-μl aliquots of successive twofold dilutions of test plasma or antibody, resuspended in medium, were added. All plasmas were heat inactivated at 56°C for 30 min before use in neutralization assays. For monkey plasma, 25 μl of a 1:10 dilution of plasma was mixed with 75 μl of the test virus. This constituted a 1:40 dilution in the representative graph. Virus equivalent to 2.5 ng of p27 capsid protein in a total volume of 75 μl of R10 was then added to each well in columns 3 to 12. Virus-free medium was added to each well in columns 1 and 2 (mock infection). The plate was incubated for 1 h at 37°C. Following this incubation, 8,000 C8166-45 LTR-SEAP cells resuspended in 100 μl of R10 were added to each well. The plate was placed in a humidified chamber within a CO_2 incubator at 37°C for 3 to 7 days. SEAP activity was measured. Neutralizing activities for all antibodies and plasma samples were measured in triplicate using a Victor V multilabel counter (Perkin-Elmer, Norwalk, CT) and reported as the average percent SEAP activity.

RESULTS

Stringent strain-specific neutralization of SHIV DH12 and SHIV KB9. The choice of SHIV DH12 and SHIV KB9 as representative viruses in this study was based on several factors: (i) both SHIVs are well-characterized, genetically modifiable molecular clones; (ii) positive plasmas from monkeys infected with the matched molecular clones over several time points postinfection were available; and (iii) positive plasmas from infected animals displayed extremely stringent strain-specific neutralizing activity.

To assess the specificity of the neutralizing activity present in monkeys infected with SHIV DH12 or SHIV KB9, neutralization assays were performed using plasma samples from animals RHTPP and Rh418, collected 0, 12, and 24 weeks postinfection with SHIV DH12 and plasma samples from animals 477-99 and 481-99, collected 0, 12, and 24 weeks postinfection, with SHIV KB9 (Fig. 1). Assays performed with plasma collected prior to infection (week zero) demonstrated no preexisting nonspecific neutralizing activity for either SHIV DH12 or SHIV KB9. Highly strain-specific neutralizing activity was ob-

TABLE 1. Neutralization of SHIV-DH12 chimeras with positive plasmas

Animal	Infecting SHIV	Time point of sera (wk)	KB9 wt[a,b]	Neutralization activity for SHIV-DH12 and DH12-derived chimeric virus[b]					
				DH12 wt	DKV12	DKV3	DKV4	DKV124	DKV1234
RHTPP	DH12	10	–	9,000	–	ND	12,000	–	–
		12	–	7,000	–	ND	15,000	–	–
		24	–	2,000	–	ND	7,500	–	–
Rh418	DH12	12	–	20,000	–	ND	20,000	–	40
		24	–	10,000	–	ND	10,000	–	–
477-99	KB9	12	2,500	–	15,000	ND	40	20,000	8,000
		24	5,000	–	8,000	ND	–	9,000	7,000
481-99	KB9	12	1,000	–	130	ND	–	300	420
		24	1,100	–	650	ND	40	1,100	800

[a] wt, wild type.
[b] The numbers indicate the reciprocals of the dilutions of plasma required to reduce the infectivity of the indicated viruses by 50%. –, 50% neutralization was not achieved, even at the lowest dilution (highest concentration) of plasma tested. ND, not determined due to inadequate infectivity of designated viruses.

served in plasma samples collected from all four experimentally infected monkeys at 12 and 24 weeks postinfection. Plasma from animals RHTPP and Rh418, infected with SHIV DH12, showed extensive neutralization of SHIV DH12 yet had no effect against the heterologous SHIV KB9 (Fig. 1A and B, respectively, and Table 1). Conversely, plasma from monkeys 477-99 and 481-99, infected with SHIV KB9, strongly neutralized SHIV KB9, but not SHIV DH12 (Fig. 1C and D, respectively, and Table 2). Most or all of the neutralizing activity was accounted for by purified immunoglobulin fractions, indicating that the neutralization was antibody mediated (data not shown).

Further studies were directed at determining whether the variable loops in gp120 were principally responsible for the strain specificity of the neutralizing antibody response and, if so, which variable loop or loops were primarily involved.

Construction of recombinant variable-loop chimeric SHIVs. SHIV DH12 and SHIV KB9 were originally constructed using SIVmac239 as the backbone and differ genetically in the *env*, *tat*, *rev*, *vpu*, and *vpr* genes, which are derived from multiple different HIV-1 species (47, 79, 86). Gp120 envelope sequences outside of the variable loops share an 82% amino acid identity between these two SHIV clones. Within the variable loops, however, homology is dramatically reduced, maintaining only 58% amino acid identity (Fig. 2A). To investigate the extent to which the variable loops of gp120 contribute to the strain restriction of the neutralizing antibody response, each variable-loop sequence was exchanged alone or in combination with other loop sequences between SHIV DH12 and SHIV KB9 (Fig. 2B). The nomenclature of each SHIV-derived variable-loop chimera reflects this construction. For each variable-loop chimeric virus, the backbone SHIV envelope sequence is identified by the first abbreviated letter (D for SHIV DH12 and K for SHIV KB9), the SHIV clone from which the exchanged variable loop was derived is indicated by the second letter, and the exchanged variable loop is identified by the numerical designation of the loop sequence. For example, SHIV DKV12 was constructed in the SHIV DH12 background to contain the V1/V2 loop derived from SHIV KB9. Virus stocks were generated by HEK 293T cell transfection, and equivalent p27 quantities were used for all comparative experiments.

TABLE 2. Neutralization of SHIV-KB9 chimeras with positive plasmas

Animal	Infecting SHIV	Time point of sera (wk)	DH12 wt[a,b]	Neutralization activity for SHIV-KB9 and KB9-derived chimeric virus[b]					
				KB9 wt	KDV12	KDV3	KDV4	KDV124	KDV1234
RHTPP	DH12	10	9,000	–	ND	–	–	ND	3,000
		12	7,000	–	ND	–	–	ND	5,000
		24	2,000	–	ND	–	–	ND	2,000
Rh418	DH12	12	20,000	–	ND	–	–	ND	10,500
		24	10,000	–	ND	–	–	ND	5,300
477-99	KB9	12	–	2,500	ND	5,000	5,000	ND	80
		24	–	5,000	ND	5,000	10,000	ND	100
481-99	KB9	12	–	1,000	ND	1,500	1,280	ND	–
		24	–	1,100	ND	1,280	1,280	ND	–

[a] wt, wild type.
[b] The numbers indicate the reciprocals of the dilutions of plasma required to reduce the infectivity of the indicated viruses by 50%. –, 50% neutralization was not achieved, even at the lowest dilution (highest concentration) of plasma tested. ND, not determined due to inadequate infectivity of designated viruses.